Formation of Fouling Layers in Wavy-Walled Channels

Ali Roustaei[1] and Ian Frigaard [1]

[1]University of British Columbia, Vancouver, BC, Canada.

ABSTRACT

We present new results on fouling layers in duct flows of yield stress fluids. By *fouling* we mean that the fluid becomes stationary in layers attached to the wall of the duct. We carry out an extensive computational study of these flows, which are characterised in the simplest scenario by 3 dimensionless parameters, $(h,\delta,,B)$. Stationary fouling layers develop if the dimensionless amplitude of the wall perturbation h exceeds some critical value h_f. Fouling can occur over a range of channel aspect ratios δ, and progressively at larger Bingham number, B. The onset occurs at a value of $(h\delta)$ that varies mainly with B. We have developed empirical expressions that give both necessary and sufficient conditions for fouling to occur.

INTRODUCTION

Fouling is often associated with physicochemical changes in the fluid in the flowing fluid, e.g. dried deposits of milk solids[1,2] or precipitation of asphaltene deposits[3,4]. Here we only consider the combination of rheological and geometric causes of fouling. Neither effect alone is able to cause fouling. Flow of a yield stress fluid along a uniform plane channel or circular pipe exhibits maximal shear stress at the wall with unyielded fluid is found only in the centre of the duct. Equally, Newtonian fluids flowing in uneven ducts do not form stationary layers, although recirculatory regions develop. In order for fouling to occur in a wavy-walled duct flow of a yield stress fluid it is intuitive that a sufficiently large amplitude of perturbation from a uniform geometry is needed. Two important situations where such variations are likely are: (i) in the processing of food pastes through machinery; (ii) in the construction of oil and gas wells.

In the first case, where geometric non-uniformities exist there is the risk of dead-zones appearing in the flow, which become sites for bacterial growth. In the second case, residual drilling mud deposits can compromise well security and later production, by allowing seepage between fluid bearing zones

The objective of our study is to begin to systematically understand geometric effects on fouling with yield stress fluid flows. We take the simplest non-trivial case, of a Bingham fluid in Stokes flow along a channel with a sinusoidal wavy-wall, as studied in previous work[5,6] for long-thin wavy-walled channels. The geometry is described by a wavelength and amplitude of the wall oscillation and by the channel width; see Fig. 1. We carry out an extensive computational study of these flows, which are characterised by 3 dimensionless parameters. We give the main qualitative features of these flows and show how the onset of fouling varies.

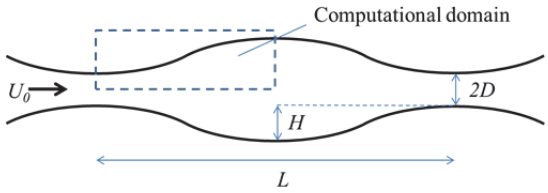

Figure 1. Geometry of a periodic wavy-walled channel

MODEL

In the geometry of Fig. 1, a Bingham fluid is pumped at mean velocity U_0 along the channel. We consider a Stokes flow and therefore may assume symmetry conditions on the flow to reduce the size of computational domain. The problem is made dimensionless using D as a length-scale, U_0 as a velocity-scale and $(\mu U_0)/D$ as the stress scale. The dimensionless equations of motion are:

$$0 = -\frac{\partial p}{\partial x} + \frac{\partial \tau_{xx}}{\partial x} + \frac{\partial \tau_{xy}}{\partial y} \quad (1)$$

$$0 = -\frac{\partial p}{\partial y} + \frac{\partial \tau_{yx}}{\partial x} + \frac{\partial \tau_{yy}}{\partial y} \quad (2)$$

$$0 = \frac{\partial u}{\partial x} + \frac{\partial v}{\partial y} \quad (3)$$

$$\tau_{ij} = \left(1 + \frac{B}{\dot{\gamma}}\right)\dot{\gamma}_{ij} \Leftrightarrow \tau > B, \text{else } \dot{\gamma} = 0 \quad (4)$$

Here $B=\tau_Y D/(\mu U_0)$is the Bingham number, (τ_Y is the yield stress and μ is the plastic viscosity). Two dimensionless parameters are defined from the geometry: $\delta=D/L$ and $h=H/L$, which we refer to as the channel aspect ratio and wall perturbation amplitude, respectively.

Equations (1)-(4), with appropriate boundary conditions are discretised using a finite element method and solved using an augmented Lagrangian method, via the freely available code Rheolef[7]. This uses an adaptive meshing technique to capture the yield surface positions and computes exactly zero rate of strain in unyielded plug regions. Details of the implementation and further computations are given elsewhere[6,8].

RESULTS

Typical examples of our results are shown below in Figs. 2 & 3, which shows a typical sequence of flows as the amplitude h is progressively increased. The speed is shown in Fig. 2 together with the flow streamlines. We observe that even the streamlines are near-parallel for small h, but soon diverge with expanding channel. Two regions of noticeably parallel streamlines are observed in the channel centre and there is no flow close to the upper wall for $h=2,4$, in the widest part of the channel.

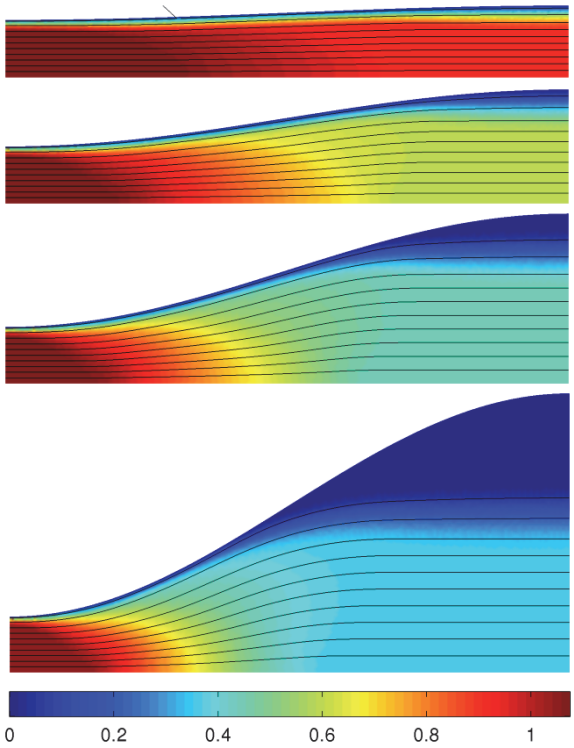

Figure 2. Variations in fluid speed and streamlines as h is increased for $\delta=0.05$, $B=20$. From top to bottom: $h=0.25, 1, 2, 4$.

In the widest part of the channel the flow has become stationary, in a layer that remains stuck to the wall, i.e. fouling. This is clearer in Fig. 3, where we plot the pressure field for the same simulations, explicitly marking the unyielded plug

regions that have been computed. At small enough h, we see that the two plugs in the centre of the channel are separated by a region of extensional flow. We see that the onset of fouling occurs in this case for $h<2$.

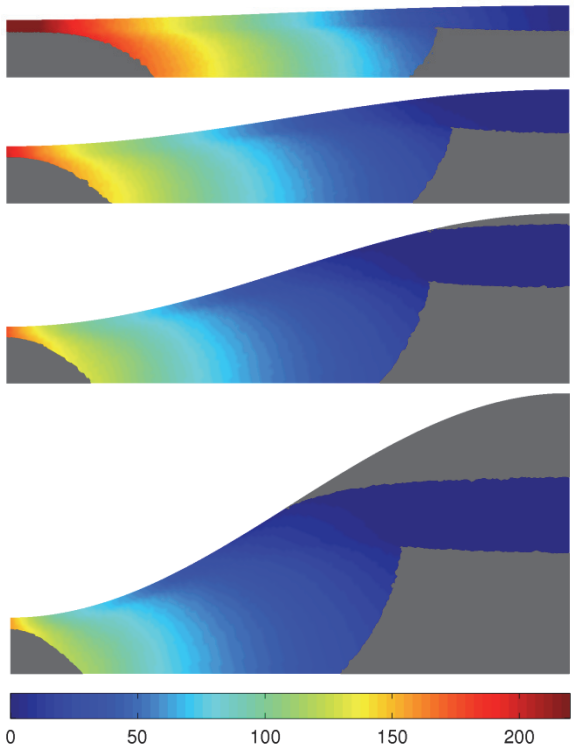

Figure 3. Variations in pressure as h is increased for $\delta=0.05$, $B=20$. From top to bottom: $h=0.25, 1, 2, 4$.The shaded grey areas denote rigid plugs

There are many interesting features of these flows, once the fouling layer appears. For example, in Fig. 3 if we focus on the yielded region between the two plugs in the widest part of the channel, it appears that there is no pressure gradient driving the flow. Closer examination reveals that this part of flow is in fact characterised by $\sigma_{yy}=0$. The shear stress τ_{xy} appears to vary quadratically across the yielded layer.

In the full paper[8], we present a fuller analysis of this region, including similarity scalings that allow us to characterise the width of yielded flow region. We also attempt to reconstruct the stress and velocity field analytically.

We have carried out a large number of computations (around 500) covering a wide range of (h,δ,B). Figure 4 shows a panorama of the different unyielded plug shapes, as (h,δ) vary, at fixed $B=20$. This helps to build up some intuition on how fouling layers vary. For the geometry considered these always form at the widest part of the channel. The formation mechanism requires that the axial gradient of extensional stress change sign as we approach the upper wall.

Once formed, increasing h appears to have minimal effect on the width of yielded region and general shape of the fouling layers in the widest part of the channel, i.e. the flow geometry self-selects and become independent of the precise shape of channel behind the fouling layer. As an example, Fig. 5 shows computations of the plug shapes in 2 channels of different shapes after significant fouling. The depth and shape of the fouling layer is very similar, as is the shape of the central plug region.

Figure 4 suggests that some combination of $(h\delta)$ is responsible for the onset of fouling. We can also see that 4 qualitatively different flow types occur. The central plug may be broken, or not. The fouling layer may be present, or not. For channels of small aspect ratio δ, the transition between broken and intact plugs at the centre of the channel is fairly well understood[5,6], and can be reasonably predicted. It is noteworthy that in shorter channels the central plug is more likely to remain intact. Equally, note that if the central plug remains intact, then it is widest in the narrowest part of the channel, which is counter-intuitive from the perspective of a momentum balance. Figure 6 plots the classification of Fig. 4 into broken/intact and fouling/no-fouling. The critical behaviour that we are interested in is the onset of fouling, which we see occurs approximately for $(h\delta) > 0.08$.

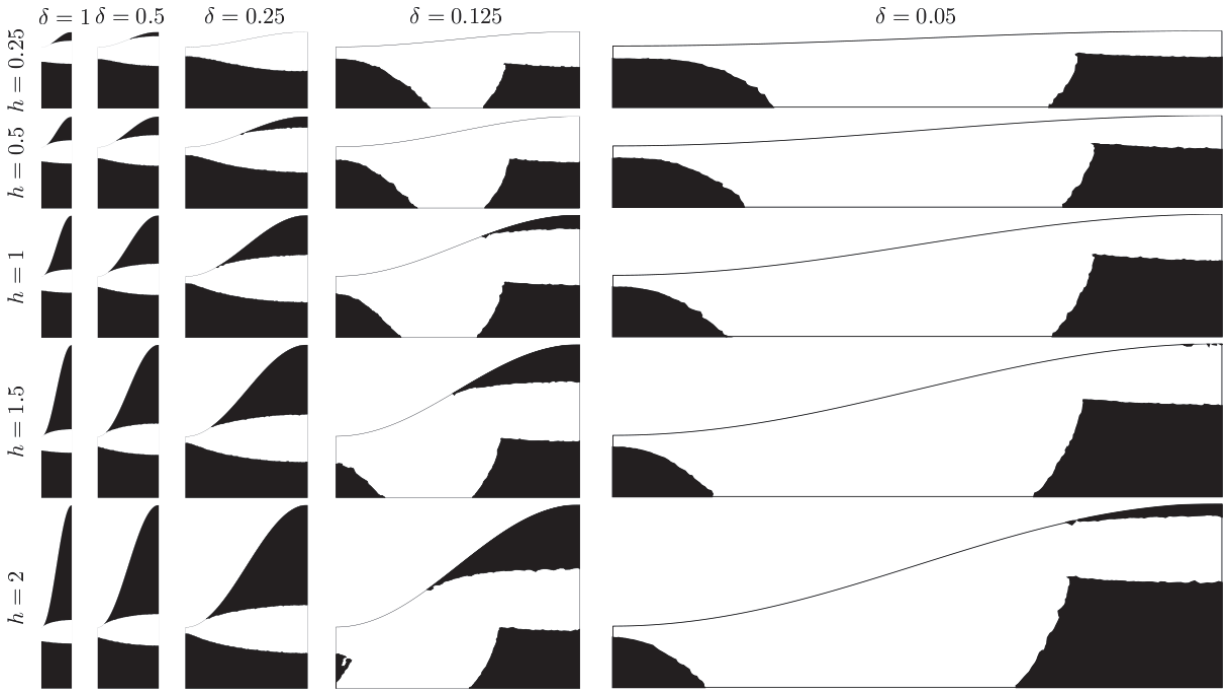

Figure 4. Panorama of different plug shapes computed at *B=20*.

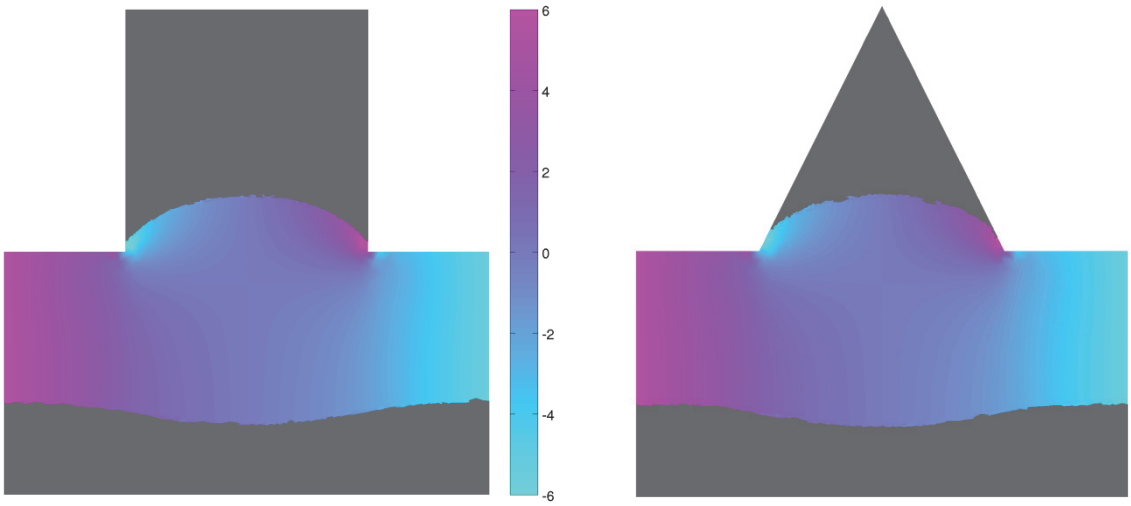

Figure 5. Pressure contours and plug shapes computed at *B=20, δ=0.5, h=1,* for 2 different shapes of wall perturbation.

We have analysed our results in a similar way over the full range of Bingham numbers computed: *0<B<100*. For each *B* we appear able to be able to find critical values of (*hδ)* that separate fouling from no-fouling. In Fig. 7 we plot all of our data in the plane *B*vs(*hδ)*. This reveals that there is only a weak dependency on geometry, other than through (*hδ),* in determining the transition to fouling.

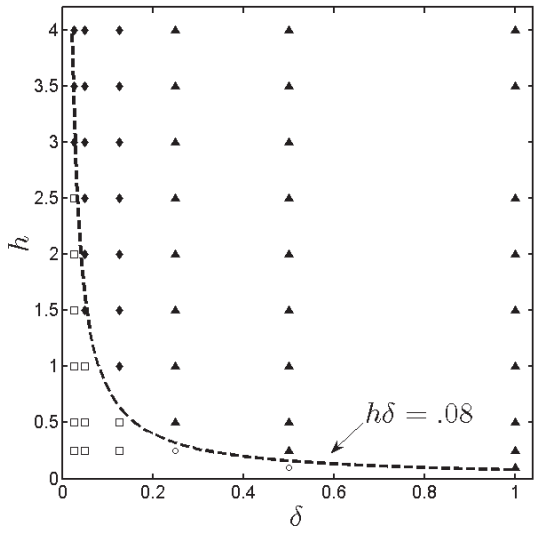

Figure 6. Data at B=20. The filled symbols denote fouling layers: diamonds denote broken central plugs and triangles intact central plugs. Empty symbols denote no fouling: squares have broken central plug and triangle intact central plug.

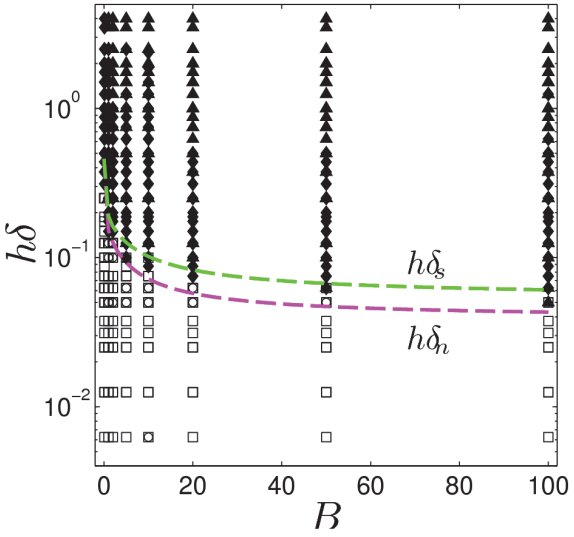

Figure 7.Partial collapse of all our data, plotting B against $h\delta$. Symbols as in Fig. 6. The two curves are defined in (5) and (6).

Instead of a single curve denoting the transition, it appears that two curves may be defined, denoting both necessary and sufficient conditions for fouling. The curves plotted in Fig. 7 are given by the following expressions.

$$h\delta_s = \frac{0.054B^2 + 1.03B + 0.31}{B^2 + 5.67B + 0.66} \qquad (5)$$

$$h\delta_n = \frac{0.039B^2 + 0.55B + 0.07}{B^2 + 3.21B + 0.15} \qquad (6)$$

Finally the limit of small Bingham number is very interesting.

Similar flows have been studied numerically[9]with one wavy wall and one plane wall. For sufficiently large hδ, instead of stationary regions recirculatory vortices appear. As the amplitude is increased, secondary vortices can form and an analogy can be drawn between these flows and classical corner vortex flows[10]. As with the corner vortices, the length-scale and intensity of the eddies decay significantly with each successive vortex.

Fig. 8 shows streamlines and unyielded plug regions for $\delta=0.5$, $h=2.5$, and sequence of increasing small $B=0$. The Newtonian limit has two recirculating vortices (Fig. 8a), but even for very small B the secondary vortex has insufficient strength to break the yield stress (Fig. 8b). As B is increased we see that the fouling layer grows outwards and a second plug is present in B the primary vortex. Further increases in B see the plug grow (Figs. 8c-e) until eventually the primary vortex is also frozen and stationary (Fig. 8f).

At the actual onset of the Newtonian recirculation, e.g. as h is increased, we do have zero shear stress in the Newtonian solution at the widest part of the channel. This implies that the onset also leads to formation of a fouling layer at any given B. However, (a small range) of larger amplitudes can then see the fouling layer disappear, replaced by a plug within a recirculating vortex!

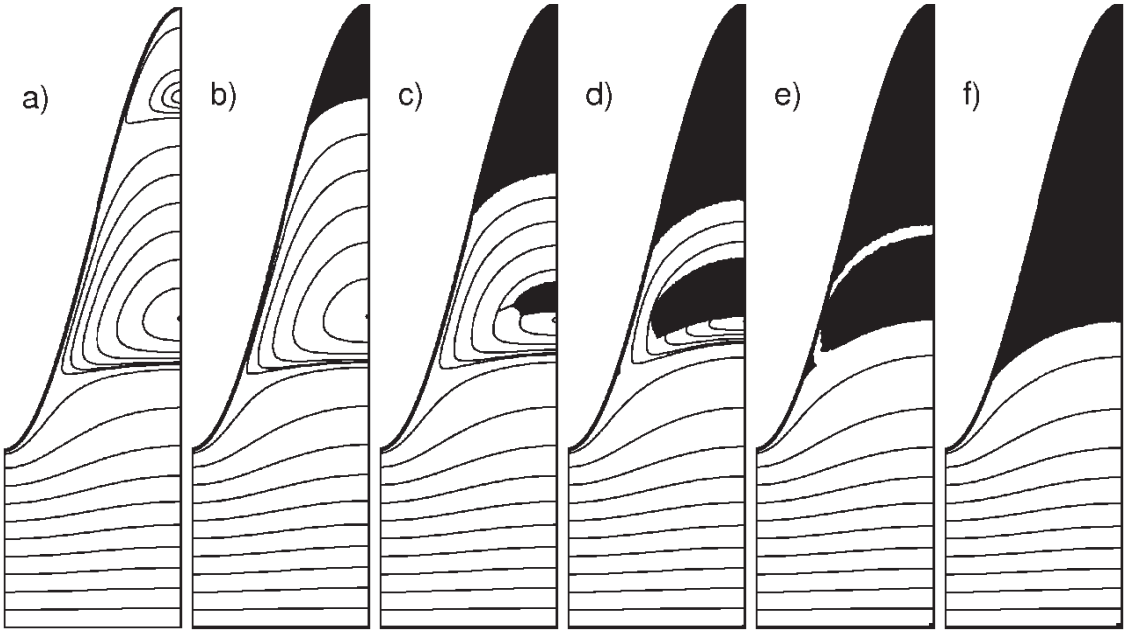

Figure 8. Streamlines and unyielded plug regions for $\delta=0.5$, $h=2.5$: a) $B=0$; b) $B=0.001$; c) $B=0.005$; d) $B=0.009$; e) $B=0.012$; f) $B=0.013$;

SUMMARY

We have carried out an extensive computational study of Stokes flows of a Bingham fluid along a wavy-walled channel. These flows are characterised by 3 dimensionless parameters, (h,δ,B). The main conclusions are as follows.

- Stationary fouling layers develop if the dimensionless amplitude of the wall perturbation h exceeds some critical value h_f.
- Fouling can occur over a range of channel aspect ratios, δ, and progressively at larger Bingham number, B.
- The onset occurs at a value of $(h\delta)$ that varies mainly with B.
- Empirical expressions have been developed that give both necessary and sufficient conditions for fouling to occur.
- The limit of large B appears to plateau to constant values of $(h\delta)$.
- At moderate B, for $h > h_f$ the fluid appears to self-select the flowing region, i.e. the shape of the fouling layer.
- Fouling at small B coincides with the onset of recirculation in Newtonian fluid flows.
- As with Newtonian flows it is theoretically possible to have secondary vortices appearing as the amplitude increases, but computationally these are hard to resolve as the stress fields are insufficient to break the yield stress.

Future directions will consider different channel geometries and the inclusion of inertia in our computations.

ACKNOWLEDGMENTS

This research was sponsored by NSERC, funding which is greatly acknowledged. We thank Pierre Saramito for his advice on using Rheolef.

REFERENCES

1. P.A. Cole, K. Asteriadou, P.T. Robbins, E.G. Owen, G.A. Montague, P.J. Fryer, Comparison of cleaning of toothpaste from surfaces and pilot scale pipework. *Food and Bioproducts Processing***88** (2010) 392–400.

2. G.K. Christian, P.J. Fryer, The effect of pulsing cleaning chemicals on the cleaning of whey protein deposits. *Trans. IChemE C*, **84** (2006) 320–328.

3. R.A. Almehaideb, Asphaltene precipitation and deposition in the near wellbore region: a modeling approach. *J. Petr. Sci. Eng.***42** (2004) 157-170.

4. D. Eskin, J. Ratulowski, K. Akbarzadeh, S. Pan, Modelling asphaltene deposition in turbulent pipeline flows. *Can. J. Chem. Eng.***89** (2011) 421-441.

5. I. Frigaard, D. Ryan, Flow of a visco-plastic fluid in a channel of slowly varying width*, J. non-Newt. Fluid Mech.***123** (2004) 67–83.

6. A. Putz, I. Frigaard, D.M. Martinez, On the lubrication paradox and the use of regularisation methods for lubrication flows, *J. non-Newt. Fluid Mech.***163** (2009)62–77.

7. P. Saramito. Efficient C++ finite element computing with Rheolef.CNRS-CCSD ed., 2012.http://wwwljk.imag.fr/membres/Pierre. Saramito/rheolef/rheolef.pdf

8. A. Roustaei, I. Frigaard, The occurrence of fouling layers in the flow of a yield stress fluid along a wavy-walled channelPaper accepted for publication in *J. non-Newt. Fluid Mech.* March 2013, to appear.

9. C. Pozrikidis, Creeping flow in two-dimensional channels, J. Fluid Mech. **180** (1987) 495–514.

10. H.K. Moffatt, Viscous and resistive eddies near a sharp corner, J. Fluid Mech. **18** (1964) 1–18.